Catalysis Letters Vol. 78, Nos. 1–4, March 2002 (© 2002)

Catalysts for combustion containing tin and copper overloaded on ZSM-5 zeolite

Piotr T. Wierzchowski * and L. Wieslaw Zatorski

IChO PAN, Institute of Organic Chemistry, Polish Academy of Sciences, Kasprzaka 44/52, 01-224 Warsaw, Poland

Received 26 June 2001; accepted 3 October 2001

Three samples of modified HZSM-5 zeolite with tin and copper were prepared by ion exchange and coprecipitation under basic conditions. The catalytic activity of prepared catalysts was tested in CO and methane combustion after pretreatments done at 873, 1088 and 1273 K. The XRD analysis and TG-DTA were used to interpret thermal stability of catalysts. Introduction of tin as the third element to well-known copper-overloaded ZSM-5 combustion catalysts improves their thermal stability. It was found that CO combustion is independent of the zeolite structure and probably adjacent sites are necessary to activate carbon monoxide and oxygen in the vicinity. Contrarily, non-dehydroxylated zeolite is indispensable as an active element together with copper or tin to catalyze methane combustion.

KEY WORDS: copper; tin; ZSM-5 zeolite; combustion; methane; carbon monoxide; thermal stability

1. Introduction

It was shown that SnO_2–CuO gels are active catalysts for the low-temperature oxidation of carbon monoxide [1]. It is known that Cu-overloaded ZSM-5 zeolite has very good catalytic activity for hydrocarbons and carbon monoxide combustion [2,3]. However, these catalysts are not thermally stable [1,4]. This disadvantage limits their use as combustion catalysts frequently exposed on thermal shocks. We have decided to examine thermal resistance of tin, copper and mixed tin–copper ZSM-5 zeolite for carbon monoxide and methane catalytic combustion.

2. Methods

2.1. Preparation of the catalysts

Tin- and copper-modified ZSM-5 zeolite catalysts were prepared by ion exchange followed by precipitation under basic conditions. The parent ZSM-5 zeolite was synthesized by an established hydrothermal procedure by means of tetrapropylammonium ions as template [5] and subsequently ion exchanged with an excess of 0.5 N HCl at 373 K. Analysis of Na and Al contents followed by the measurement of cation exchange capacity of ammonium ions (0.5 N NH_4Cl; pH $=$ 7.0; two-fold 2 h; 373 K) allowed one to estimate the chemical formula $Na_{0.03}H_{1.61}Al_{1.64}Si_{94.36}O_{192}\cdot 0.53Al_2O_3$. Ion exchange capacity of this sample was equal to 0.28 meq g^{-1}. From the morphological point of view, it is composed of well-defined crystallites of dimension 0.2×2 μm and their aggregates.

Copper and tin were introduced to the H form of zeolite by ion exchange and precipitation under basic conditions. The samples, each of 5 g of zeolite, were introduced to 50 cm^3 of freshly prepared clear solutions of copper nitrate (0.5 M), tin tetrachloride (0.5 M) or to 50 cm^3 of the solution combined from two equal portions of the formers.

The suspensions were stirred 1 h at room temperature and then heated to 323 K. Each 0.5 h, pH was increased by 0.5 unity by adding 3 M NH_4OH solution up to the value shown in table 1. The samples were then washed and filtered, followed by drying at 393 K for 5 h.

The specimens of 0.5 g of the prepared zeolites have been further calcined in air at 873, 1088 and 1273 K. The final temperature was reached with a ramp of 10 K min^{-1} and hold for 15 min.

2.2. Characterizations

Tin and copper content were established by inductive coupled plasma (ICP) analysis. Table 1 compiles the list of materials with final pH of metal deposition and reached metal content.

Thermogravimetry and differential thermal analyses were obtained using a Paulik–Paulik–Erdey Q-1500 derivatograph.

The crystallinity of calcined samples was established by collecting X-ray diffractions on a Rigaku-Deneki diffractometer using Cu Kα radiation. The zeolite crystallinity estimation was done by comparing the sum of absolute intensities of 131, 430, 151, 303 and 432 reflexes assigned to space group Pnma.

TPD of isopropylamine (IPA) was applied for measuring Brønsted acidity of samples according to the method introduced by Gorte [6]. This method is based on the assumption that IPA chemisorbed on Brønsted acid sites (BAS) undergoes Hoffman elimination to propylene. In TPD-TGA experiment the sample of zeolite (40 mg) was heated to

---

* To whom correspondence should be addressed. E-mail: piowie@icho.edu.pl

Table 1
List of prepared zeolite samples

Catalyst	Metal content ($mmol\,g^{-1}$)			Acidity ($mmol\,g^{-1}$)			
	pH	Cu	Sn	Noncalcined		Calcined at 1088 K	
				Total[a]	BAS[b]	Total[a]	BAS[b]
CuZSM-5	8.0	0.71	–	0.430	0.204	0.441	0.048
SnZSM-5	7.1	–	0.87	0.487	0.261	0.345	0.102
Cu/SnZSM-5	7.2	0.45	0.45	0.376	0.240	0.407	0.201

[a] Determined as irreversibly adsorbed IPA at 430 K.
[b] Determined as IPA which undergoes Hoffman elimination during desorption.

750 K (12 $K\,min^{-1}$) in vacuum (10^{-5} Torr) on a Cahn RG Electrobalance® for removing water and then exposed to 1–2 Torr of IPA at room temperature. After evacuation (10^{-5} Torr) at 430 K total chemisorption of IPA was established, then the temperature was ramped 12 $K\,min^{-1}$ to 750 K. The sample weight returned to its initial value at this temperature. The desorbed IPA and propylene were collected in a liquid nitrogen trap. Finally, the gases from the trap were analyzed with a mass spectrometer (AMD 604) using the peak intensities at $m/e = 44$ for IPA and the sum of peak intensities at $m/e = 39$ and 41 for propylene. The mass spectra analysis of volumetrically prepared standards (covering the entire range of IPA to propylene proportions found in the experiments) was used to calibrate the spectrometer response. The results obtained by mass spectrometry of collected desorbants are closely related to the mass losses observed during desorption in the range of 610–690 K.

2.3. Catalytic tests

The catalytic activities of zeolites in the combustion of methane and carbon monoxide were determined using a fixed-bed reactor and supplying oxygen in a stoichiometric ratio. The experimental setup consisted of the pressure regulators, mass flow controller and temperature controller-programmer connected to a vertical tube furnace.

The reactions were carried out in a tubular quartz reactor (4 mm inner diameter). Temperature was measured before the catalyst bed. The reaction mixtures were prepared in the pressure cylinders. Special attention was paid to elimination of a segregation of the mixtures caused by gravity with the help of thermal convection imposed in the cylinder.

The catalysts were pressed, crushed and sieved to a fraction of 0.10–0.63 mm. The sample of 0.2 g was diluted (1 : 2) with quartz particles of the same diameter range and placed between two swabs of quartz wool in the exit part of the reactor with the inlet serving as reacting gas preheater. The reaction products were monitored using a gas chromatograph equipped with a methanizer and FID detector. The sampling system and separating column packed with Carbosieve allowed performing automatic analysis every 15 min. Data acquisition were carried out by a personal computer.

The reaction mixtures consisting of 1% of CO and 0.5% of oxygen or 1% of CH_4 and 2% of oxygen in helium balance were introduced to the reactor at a flow rate of 100 $cm^3\,min^{-1}$ and 1 atm of total pressure (WHSV = 30000 $scm^3\,h^{-1}\,g^{-1}$). For detailed kinetics measurements flow rate was changed.

Prior to combustion testing, the catalyst samples were heated in desired gas flow at a heating rate of 10 $K\,min^{-1}$ up to 873 K (or up to 673 K – only in the case of non-calcined samples). Standard pretreatment was done using 20% of oxygen in helium; reduction was performed using 20% of hydrogen in helium. The catalysts were then cooled down to 373 K in helium flow. After stabilization of the temperature, the reagent mixture was fed to the reactor. The first test of combustion efficiency involved measurements of conversion continuously monitored in line with the temperature rise at a heating rate of 2 $K\,min^{-1}$ up to 673 K. The second test was performed in the temperature region with conversion being below 10%. In that test the conversions were measured at least at four selected temperatures and using different flow rates of the reagents. The data collected at descending temperature were used for calculation of the apparent activation energy. A fresh portion of the catalyst was used when the reagents (methane to carbon monoxide) were changed.

The blank tests were done using parent HZSM-5 zeolite as the catalyst and reaction conditions presented in figures 2 and 3. CO conversion reached 0.1% at 573 K, methane conversion at 673 K was equal to 0.09% with 40% of selectivity to carbon dioxide.

3. Results and discussion

3.1. Materials characterization

Figure 1 shows TG-DTA curves for investigated catalysts in the region ambient – 1273 K. The X-ray powder diffraction data obtained for the calcined catalysts are summarized in table 2. After calcination of all investigated catalysts at 873 K the XRD pattern shows only the zeolite phase of ZSM-5 crystallized in the space group Pnma. Very small changes of relative peak intensities caused by ion exchange are observed in comparison to the parent HZSM-5 sample. In that region (ambient – 873 K) TG-DTA data shows the weight loss due to dehydration of zeolite with the endothermic DTA peak at 380 K followed by further endothermic dehydration steps. Dehydration of copper species is observed in the range of 480–580 K. The quantity of water liberated during this dehydration step is close to one water molecule per one copper ion.

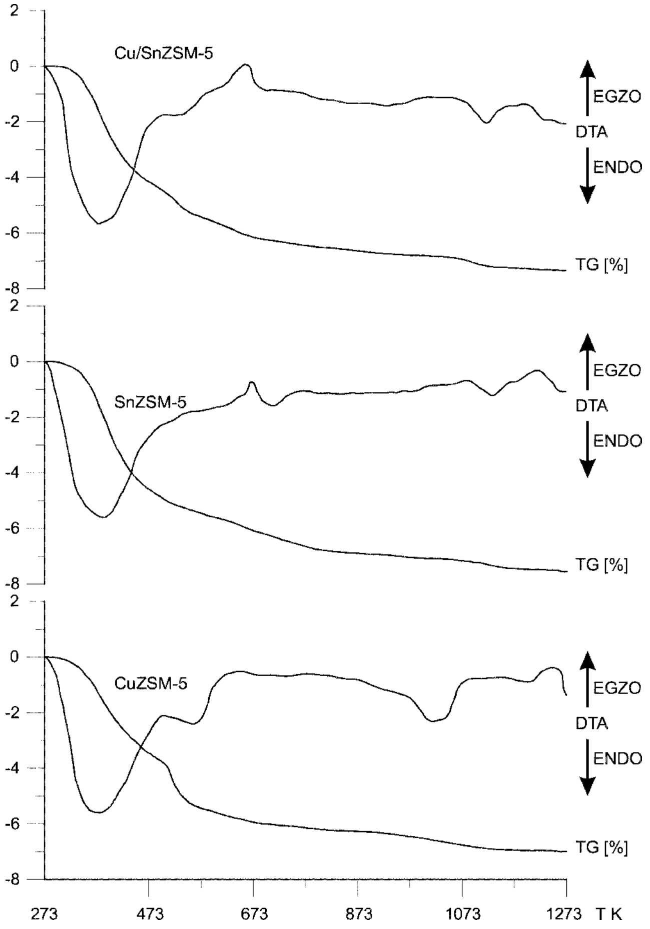

Figure 1. TG and DTA analysis of tin- and copper-containing ZSM-5 zeolites.

At 580 K all investigated samples lost the same quantity of water (5.4%) indicating that copper cations coordinate zeolitic water. The UV-vis spectroscopy of Cu^{2+}/ZSM-5 sample reported in [7] showed that dehydration of Cu^{2+} hydrated species occurs under high vacuum at lower temperature (473 K). Dehydration of tin species occurs in the range of 580–790 K. The observed amount of water liberated during dehydration of tin-containing samples in this process is approximately close to half of a water molecule per atom of tin.

The XRD analysis shows that some loss of zeolite structure crystallinity occurs after calcination at 1088 K. The most advanced collapse of zeolite structure was observed in the case of mixed copper–tin sample (about 30% of collapse) in contrast to CuZSM-5, which preserved full crystallinity. Besides the zeolite structures the XRD shows also traces of SnO_2 as broad peaks at 26.5° and 33.9° 2Θ.

In the region of 873–1088 K TG-DTA analysis of CuZSM-5 sample shows endothermic loss of mass at 1020 K. A similar effect was observed in the case of mixed copper–tin sample at the higher temperature of 1070 K and for SnZSM-5 sample at 1090 K. The observed amount of water molecules liberated during this process is close to one per two ion exchange sites of zeolite. It could be rationalized by dehydroxylation of zeolite and subsequent water elimination from copper species and formation of polynuclear $-(Cu{-}O)_n{-}Cu^{2+}$ oxycations. The formation of oxycations has been reported in the case of not overloaded CuZSM-5 zeolites during dehydration and self-reduction in vacuum or in inert gas flow [7,8]. In the case of over-exchanged CuZSM-5 zeolites the situation is much more complex. Oxycations attached to the ion exchange sites and other undefined CuO-oxidic like species are present in zeolite just after ion exchange. The remaining ion exchange sites after the applied exchange procedure are occupied by ammonium cations and form the acidic hydroxyls after calcinations. The results of acidity measurements are presented in table 1. All prepared samples exhibit high Brønsted acidity. The rehydration of calcined samples does not restore their original BAS density. This means that the dehydroxylation observed in the range 1000–1100 K is irreversible to a great extent. The lowest BAS density after calcinations at 1088 K is observed in the case of CuZSM-5 sample.

After calcination at 1273 K all samples show dramatic collapse of zeolite structure. CuZSM-5 sample entirely recrystallized in SiO_2 (tridymite) and CuO. Tin-containing samples are more stable and zeolite is still observable in

Table 2
X-ray powder diffraction data for calcined Cu- and Sn-containing ZSM-5 zeolites

Calcination temperature (K)	CuZSM-5	SnZSM-5	Cu/SnZSM-5
873	Only zeolite ZSM-5 phase detected (Pnma), full crystallinity		
1088	Zeolite 100%,[a] broad CuO pattern	Zeolite 80%,[a] broad SnO_2 cassiterite phase at 26.52°, 33.88°, 37.97° $2\ \Theta$	Zeolite 70%,[a] broad SnO_2 cassiterite pattern no CuO phase detected
1273	No zeolite detected, SiO_2 tridymite phase at 21.59°, 23.03°, 23.31° $2\ \Theta$ and sharp CuO pattern at 35.5°, 38.7°, 39.0° 2Θ	Zeolite 30%,[a] sharp SnO_2 cassiterite pattern	Zeolite 20%,[a] sharp SnO_2 cassiterite pattern no CuO phase detected

[a] Approximation was done comparing the sum of absolute intensities of 131, 430, 151, 303 and 432 (*hkl*) reflexes assigned to the space group Pnma with the intensities obtained for the parent HZSM-5 sample.

Table 3
Apparent activation energy of carbon monoxide combustion

Catalyst	E (kJ mol^{-1})
CuZSM-5	67–72
SnZSM-5	65–70
Cu/SnZSM-5	52–56

XRD analysis together with the SnO_2 (cassiterite) phase; in that case no CuO phase was detected.

3.2. Activity in the carbon monoxide combustion

All investigated samples catalyzed carbon monoxide combustion. The steady state conversions of carbon monoxide observed at 457 K are compared in figure 2 as a function of calcination temperature of catalysts. The catalysts calcined up to 873 K have very diversified activities. CuZSM-5 zeolite is the most active in carbon monoxide combustions, Cu/SnZSM-5 is more than one order of magnitude less active and SnZSM-5 is least active. Catalytic activity measurements with the different space velocities were done for the samples noncalcined and calcined at 873 K. The initial reaction rates for carbon monoxide combustion were determined as slopes of the dependence of the conversion on reciprocal space velocity at $1/\mathrm{WHSV} = 0$. The temperature dependence of initial reaction rates allowed calculating apparent activation energies, which are presented in table 3. One can observe that tin introduction as the second active element decreased activation energy of the reaction. The synergetic effect of mixed oxides containing SnO_2 in catalytic oxidation of carbon monoxide is well known [1,9]. The lower activity of Sn/CuZSM-5 catalyst (containing less copper) indicates that the unique properties of overloaded CuZSM-5 zeolites are due to the high density of active copper sites able to activate carbon monoxide and oxygen molecules in the vicinity.

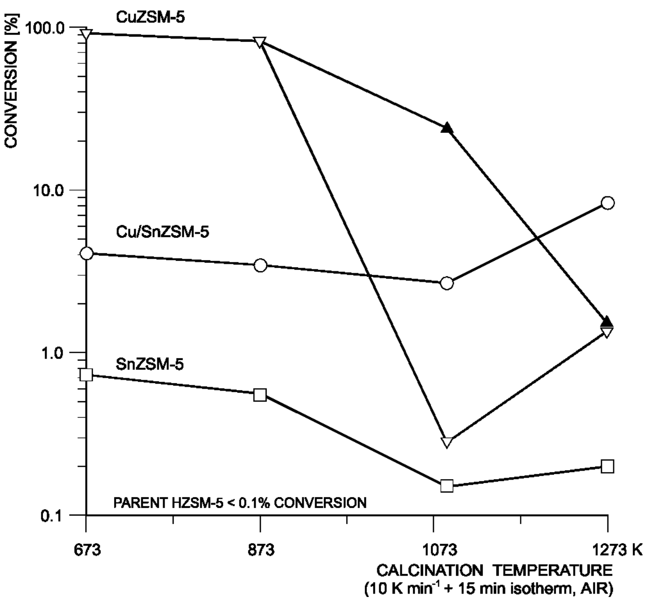

Figure 2. Oxidation of 1% CO in 0.5% O_2, helium balance, at flow rate 100 cm^3 min^{-1}, through 0.2 g of catalyst beds at 457 K as a function of calcination temperature. (▲) Conversions obtained after additional hydrogen reduction of CuZSM-5 samples at 673 K.

The catalysts calcined at 1088 and 1273 K exhibited different properties. As was expected, copper catalyst lost almost completely activity in carbon monoxide combustion after calcination at 1088 K. This behavior can be attributed to the dehydroxylation process and agglomeration of CuO oxidic like species, which independently of stabilized in zeolite quantity of Cu(I) ions caused the latter no accessibility to reagents.

Contradictory results concerning the presence and the role of Cu(I) cations in CuZSM-5 zeolite have been reported in the literature. Recently the results of EPR measurements were presented [10] indicating an insignificant presence of Cu^+ before and after selective reduction of NO with C_3H_8 even in over-exchanged CuZSM-5. In that case the catalytic activity is due to facile interconversion between Cu^+ and Cu^{2+} species. However, the formation of Cu^+ ions generally is not questioned [7]. The results of irreversible CO adsorption and XPS measurements indicate that 68% of copper has oxidation number 1+ after reduction by CO at 300 K [11].

Recently reported spectroscopic and calorimetric studies of CO adsorption on Cu(II)ZSM-5 [12,13] and Cu(I)ZSM-5 [14] indicate strong chemisorption of CO on Cu^+ cations with formation of σ-donated Cu^+–CO species. Differential heat of CO adsorption is higher than 130 kJ mol^{-1} for the most active Cu(I) zeolitic cations. This implies that both carbon monoxide and oxygen are strongly chemisorbed in ZSM-5 zeolite and they should be adsorbed in the vicinity for the surface reaction to occur. From that point of view the observed deactivation of CuZSM-5 catalyst can also be explained as elimination of one of two adjacent sites necessary for the carbon monoxide and oxygen adsorption.

Nevertheless, the CuZSM-5 zeolite after calcination at 1088 K was less active even compared to the sample with zeolite totally destroyed after calcination at 1273 K (that is to CuO on silica). An additional experiment was done to check the possibility of copper active sites regeneration. The activity in CO oxidation of CuZSM-5 calcined at 1088 K in air was restored after hydrogen treatment at 673 K and remained stable after further oxygen treatment up to 873 K. Reduction by hydrogen at 673 K is sufficient to reduce copper mostly to Cu(I) and partially to the metallic state [13,15] and SnO_2 to SnO on the surface [9]. The collapsed sample after hydrogen treatment did not restore the catalytic activity.

CuSnZSM-5 remains active after calcination at high temperatures; the sample calcined at 1273 K is the most active form of this catalyst despite partial collapse of the zeolite framework. In that case the reason for catalytic activity is probably the good dispersion of copper species on the surface of mixed tin oxide and partially destroyed zeolite.

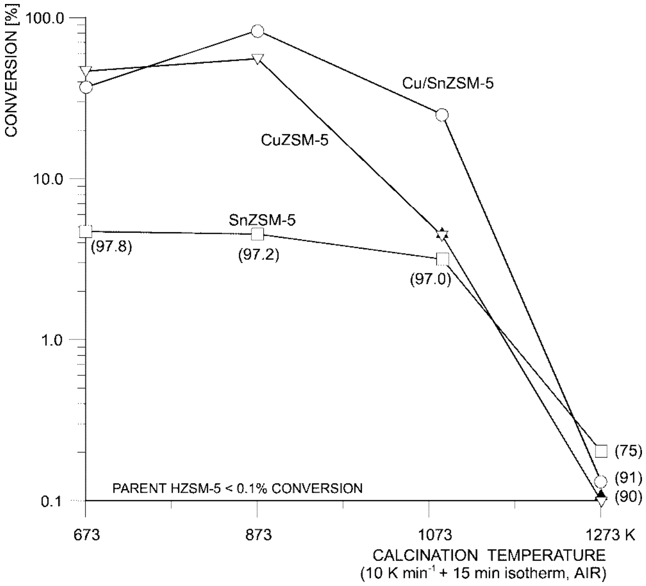

Figure 3. Oxidation of 1% CH_4 in 2% O_2, helium balance, at flow rate 100 cm^3 min^{-1} through 0.2 g of catalyst beds at 673 K as a function of calcination temperature. (▲) Conversion obtained after additional hydrogen reduction of CuZSM-5 samples at 673 K. Labels in parentheses denote percent of selectivity to carbon dioxide, for points without labels the selectivity excess 99.9%.

3.3. Activity in the methane combustion

Only catalysts calcined at temperature up to 1088 K are active in methane combustion (figure 3). Selectivity to carbon dioxide (measured at 673 K) was over 99.9% for almost all samples containing copper. Only in the case of the least active CuZSM-5 sample (calcined at 1273 K) did CO_2 selectivity decrease to 90% (at 0.16% of methane conversion). SnZSM-5 zeolite was less selective; the sample calcinated at 873 K exhibited 97.2% selectivity to CO_2 (1.3% of methane conversion at 673 K).

Samples of Cu/SnZSM-5 zeolite calcined at 873 and 1088 K are the most active in methane combustion. Methane conversion measurements with different space velocities were done for samples calcined at 873 K. The reactor was considered as an integral plug–flow reactor. The kinetic analysis indicated that the reaction is first order with respect to methane and zero order with respect to oxygen. A very good fit to the Arrhenius equation was obtained at the measured conversion level (below 10%). The results of apparent activation energy calculation are shown in table 4.

Comparing methane conversions at 673 K and apparent activation energies one can observe that tin introduction as the second active element increases the number of active centers in the catalyst.

CuZSM-5 zeolite after calcinations at 1088 K is about three times less active compared to the sample calcined at 873 K. Hydrogen treatment at 673 K followed by reoxidation did not increase the activity as it was observed in the case of carbon monoxide combustion. The role of Brønsted acid sites for methane combustion seems to be essential. The strength and quantity of BAS cannot be easily regenerated after dehydroxylation by treatments in the reduction–oxidation cycle. The role of tin in thermal resistance of the copper zeolite methane combustion catalyst could be probably due to the increasing of the dehydroxylation temperature by about 50 K as was observed on TG-DTA curves. The participation of tin in creation of additional active sites can be explained by formation of new sites capable of activating oxygen and leaving in zeolite more BAS responsible for methane activation. There is no expected competition between oxygen and methane for active sites in chemisorption and probably no adjacent sites are necessary due to the high mobility of the chemisorbed species.

Table 4
Apparent activation energy of methane combustion

Catalyst	E (kJ mol^{-1})
CuZSM-5	87.4 ± 1.5
SnZSM-5	109.3 ± 3.8
Cu/SnZSM-5	98.2 ± 1.2

4. Conclusions

The possibility of catalyst activity enhancement in methane combustion by introducing, as the third component, hydrous SnO_2 coprecipitated during cation exchange of copper in HZSM-5 zeolite was shown. Such a catalyst exhibits better thermal stability compared to the standard overloaded CuZSM-5 zeolite. Copper- or tin-containing zeolite catalyzes the methane combustion. Both copper sites and probably strong Brønsted acid sites are necessary for the catalytic activity. Copper zeolite becomes less active after dehydroxylation and cannot be regenerated by hydrogen treatment. Introduction of tin to copper zeolite increases the dehydroxylation temperature and hence its thermal stability.

It was found that carbon monoxide oxidation is independent of zeolite structure preserved after calcination and can occur also after zeolite collapse, probably on centers formed as well-dispersed copper species. The elimination of adjacent copper active sites is used to explain the known phenomenon of overloaded CuZSM-5 zeolite deactivation after calcination at elevated temperatures. Such deactivation is not permanent and catalytic activity in CO oxidation can be restored by hydrogen treatment at 673 K.

Further studies are in progress to examine the properties of tin-oxide-modified zeolite catalysts by a multitechnique investigation.

Acknowledgment

This research was partly carried out under European Commission grant INCO no. ERBIC15CT980515.

References

[1] M.J. Fuller and M.E. Warwick, J. Catal. 34 (1974) 445.

[2] J.S. Ritscher, US Patent No. 4331644 (1982).

[3] A.K. Neyestanaki, N. Kumar and L.-E. Lindfors, Fuel 74 (1995) 690.

[4] A.-Z. Ma, M. Muhler and W. Gruenert, Appl. Catal. B 27 (2000) 37.

[5] R. Mostowicz et al., Polish Patent No. 125 146.

[6] R.J. Gorte, Catal. Lett. 62 (1999) 1.

[7] G. Turnes Palomino, P. Fisicaro, S. Bordiga, A. Zecchina, E. Giamello and C. Lamberti, J. Phys. Chem. B 104 (2000) 4064.

[8] P.H. Kasai and R. Bishop, J. Phys. Chem. 81 (1977) 1527.

[9] R. Sasikala, N.M. Gupta and S.K. Kulshreshtha, Catal. Lett. 71 (2001) 69.

[10] S.A. Gomez, A. Campero, A. Martinez-Hernandez and G.A. Fuentes, Appl. Catal. A 197 (2000) 157.

[11] M.C.N. Amorim de Carvalho, F. Barboza Passos and M. Schmal, Appl. Catal. A 193 (2000) 265.

[12] Y. Kuroda, Y. Yoshikawa, S. Emura, R. Kumashiro and M. Nagao, J. Phys. Chem. B 103 (1999) 2155.

[13] A. Gervasini, C. Picciau and A. Auroux, Micropor. Mesopor. Mater. 35–36 (2000) 457.

[14] V. Bolis, S. Maggiorini, L. Meda, F. D’Acapito, G.T. Palomino, S. Bordiga and C. Lamberti, J. Chem. Phys. 113 (2000) 9248.

[15] R. Bulanek, B. Wichterlova, Z. Sobalik and J. Tichy, Appl. Catal. B 31 (2001) 13.